Chapter 9 *TWO DIMENSIONAL HOMONUCLEAR J-CORRELATED SPECTROSCOPY*

Multi-dimensional NMR experiments generate a spectrum in which the position of a spectral line, or peak, is defined by **two or more frequencies**. The existence of such a peak indicates that the participating spins are coupled to one other by scalar (J) coupling through chemical bonds or via dipolar coupling through space. The position of the peak is defined by the chemical shifts, or resonance frequencies, of the coupled spins.

Spin system: Spins, such as those in an amino acid residue belong to the same network of scalar coupled spins. (Exception : Aromatic ring has its own system due to small coupling with H_β.

➔ The spins that belong to a spin-system can be identified by multidimensional J-correlated spectroscopy. The identification of residue type on the basis of the properties of the spin system, such as the number and type of chemical shifts, is an important step in the assignment of resonance lines to individual atoms in the protein.

➔ In addition to providing information for resonance assignments, the J-coupling constants can often be extracted from these spectra, providing structural information on the torsional angles. Finally, the increased dimensionality of the experiment also increases the resolution of the spectrum, permitting the observation of resolved lines in large systems.

➔ This chapter begins with a general introduction to multi-dimensional NMR spectroscopy and then features a discussion of three important homonuclear two dimensional experiments: COSY, DQF-COSY, and TOCSY, each of which are used to elucidate scalar couplings between spins within a spin-system. Experiments that elucidate heteronuclear couplings will be discussed in Chapter 10.

Spin systems of amino acid and nucleic acids

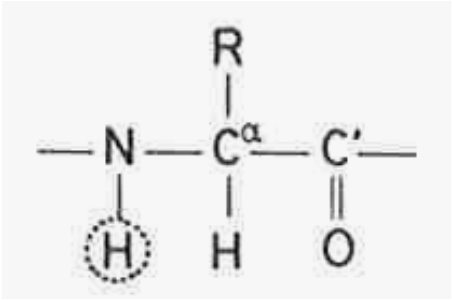

TABLE 2.2. Side Chains R (see Fig. 2.1) and Three-Letter and One-Letter Symbols for the 20 Common Amino Acids, and Spin Systems of the Nonlabile Hydrogen Atoms in the Molecular Fragments H–αC–R[a,b]

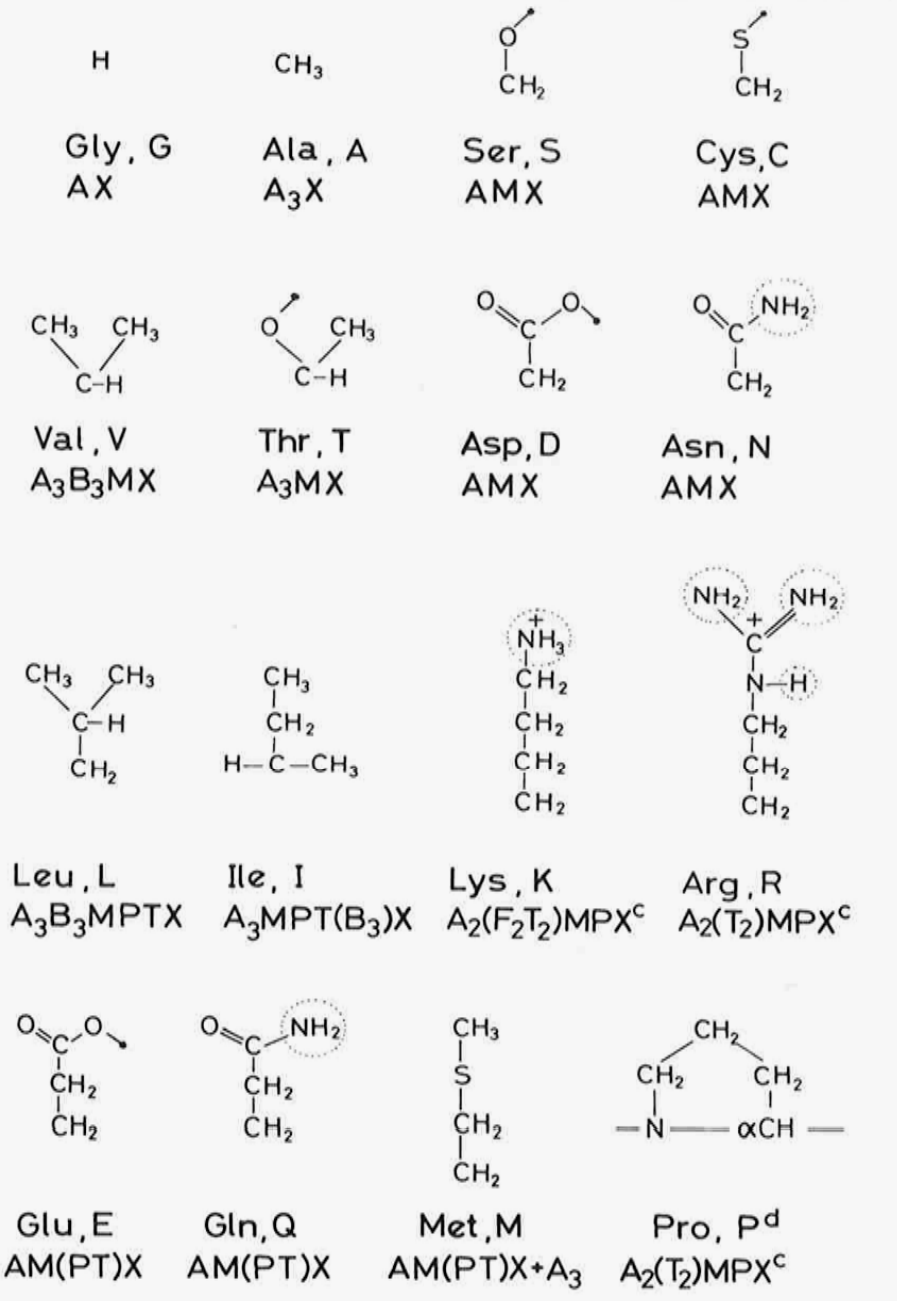

TABLE 2.2. (Continued)

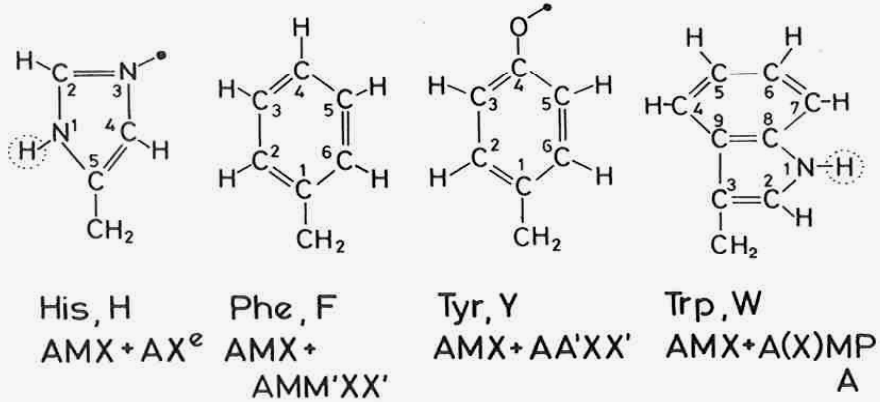

[a] Also indicated is the numeration used for the aromatic ring atoms. Not indicated is the standard identification of the other side chain heavy atoms by lower case Greek letters, with βC being next to αC (IUPAC–IUB Commission on Biochemical Nomenclature, 1970).

[b] Labile protons that can under certain conditions be observed by NMR in aqueous solution are shown in dotted circles. Those labile protons, which are not usually observed, are indicated by small filled circles.

[c] For simplicity the spin systems for Arg, Lys, and Pro were written with the assumption that with the exception of the β position, each methylene group gives rise to a single two-proton resonance.

[d] The structure for Pro includes the backbone atoms αCH and N.

[e] In His, 2H and 4H appear often as two singlet lines, but the connectivity through the small four-bond coupling of approximately 1 Hz was observed in several proteins. 2H can be exchanged with deuterium of the solvent, D_2O, within a period of several hours to several months.

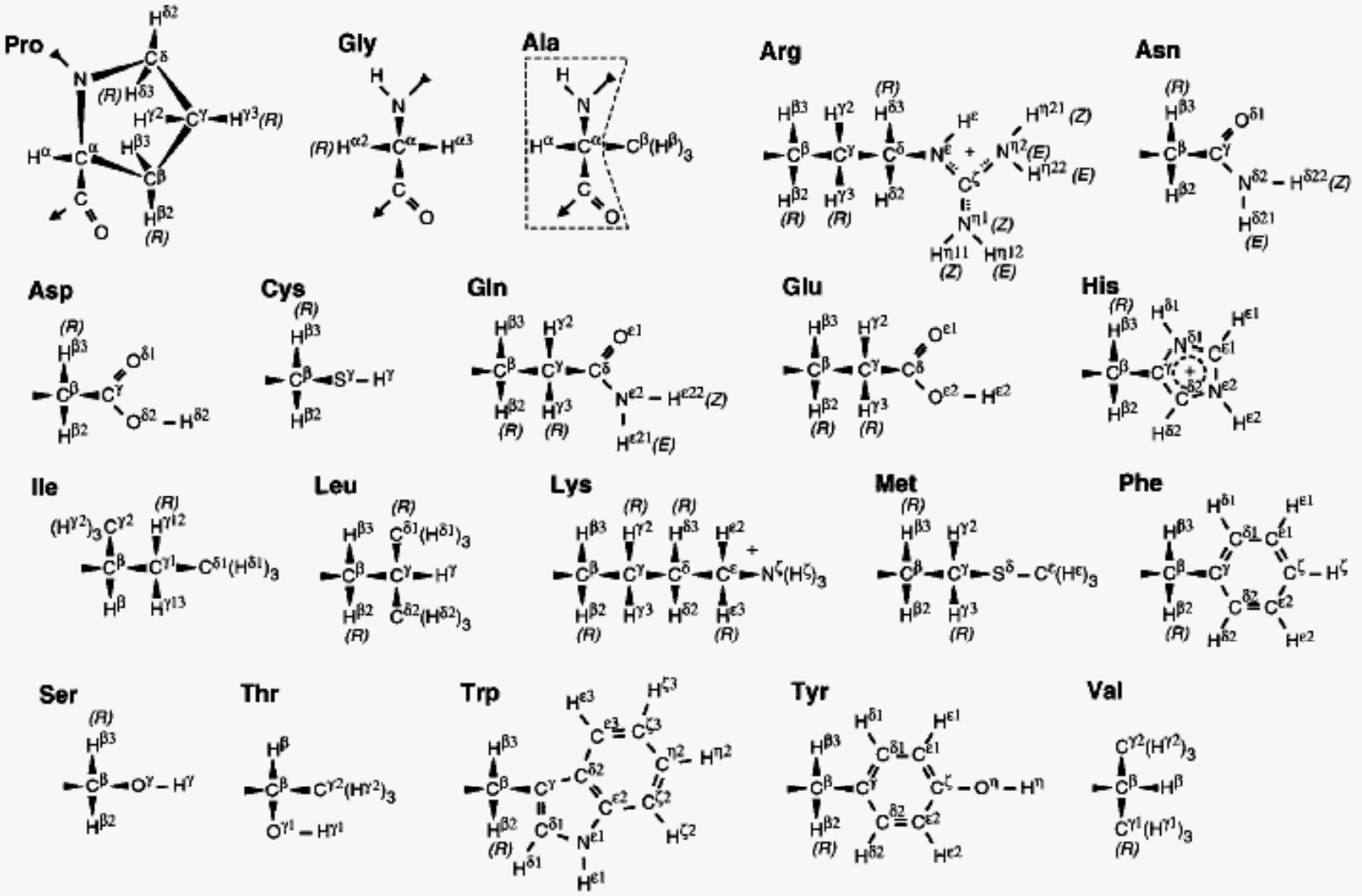

Figure 1. Recommended atom identifiers for the 20 common amino acids follow the 1969 IUPAC-IUB guidelines (ref. 20). Backbone atoms are shown for Pro, Gly, and Ala but not for the other L-amino acids (where they correspond to those bounded by the broken line in the Ala structure). Greek letters are used as atom identifiers. The C^{α} or the substituent closer to C^{α} (in the order C^{α}, C^{β}, C^{γ}, ...) takes precedence over atoms in branches in defining stereochemical

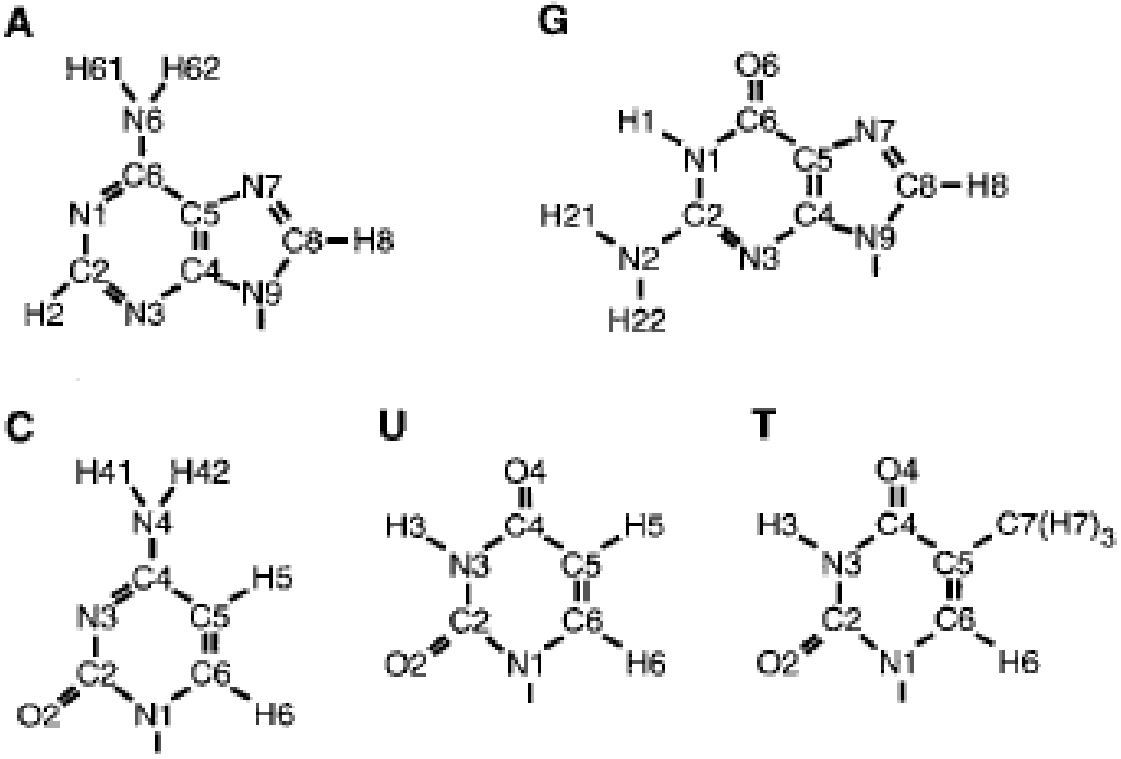

Figure 2. Nomenclature, structures, and atom numbering for the sugars and the bases contained in common nucleotides (ref. 22). The identifiers shown here for the hydrogen atoms largely follow previous recommendations as discussed in Section 2 of the text, indicater *pro-R* (*R*).

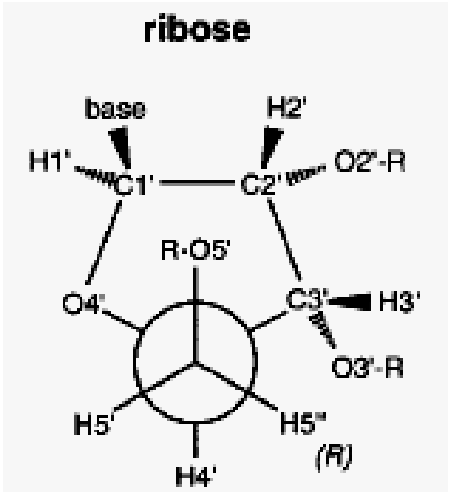

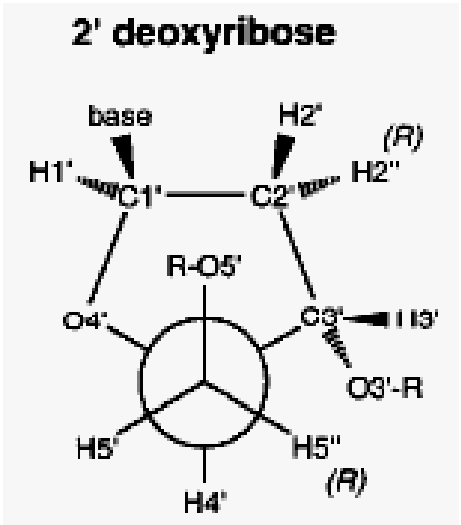

9.1 Multi-dimensional Experiments

Magnetization initially at A is transferred to B. The signal detect in B will have depends on both A and B.

$$A \longrightarrow B, \qquad S(t_1, t_2) = \eta e^{i(\omega_A t_1)} e^{i(\omega_B t_2)}$$

Fourier transform of S will contain both ω_A and ω_B (2D NMR).

Similarly one can have 3D NMR by: A → B → C and $S(t_1, t_2, t_3) = \eta e^{i(\omega_A t_1)} e^{i(\omega_B t_2)} e^{i(\omega_C t_3)}$

$$\Omega(\omega_1, \omega_2) = \int \int S(t_1, t_2) e^{i\omega t_1} e^{i\omega t_2} dt_1 dt_2$$

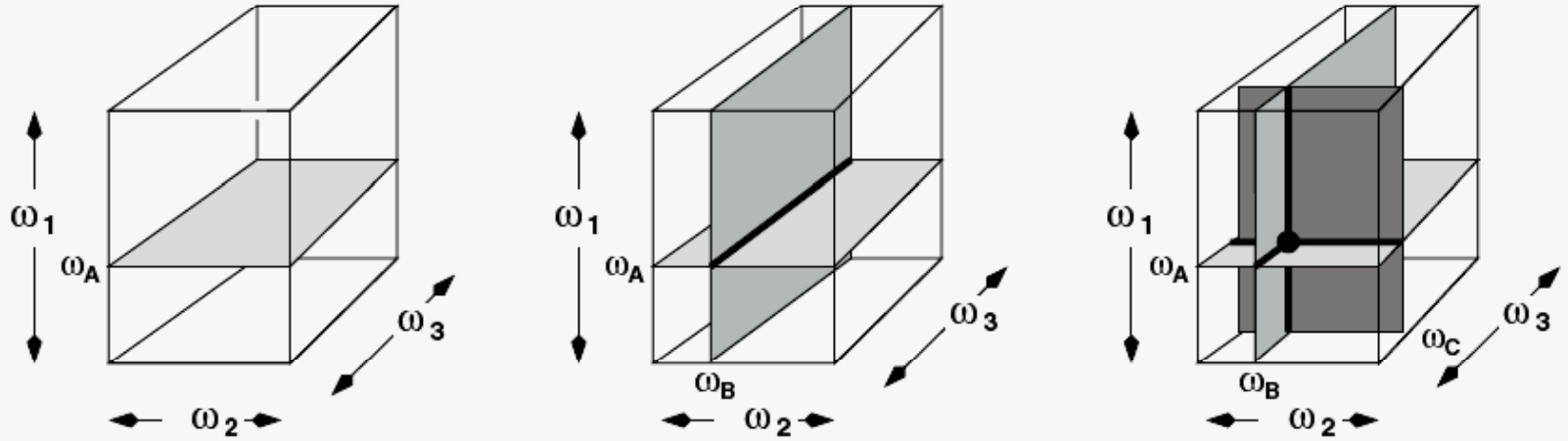

Figure 9.1. Peak location in a three-dimensional spectrum. The location of a crosspeak in a three dimensional spectrum is defined by the intersection of three orthogonal planes. The first plane is the locus of all points that have a frequency of ω_A in the first frequency dimension. The second plane is the locus of all points that have a frequency of ω_B in the second frequency dimension. The intersection of these two planes is a line, as indicated in the center diagram. The third plane is defined by all points that have a frequency of ω_C in the third frequency dimension. This plane intersects the line at a single point, which is location of the crosspeak.

9.1.1 Elements of Multi-dimensional NMR Experiments

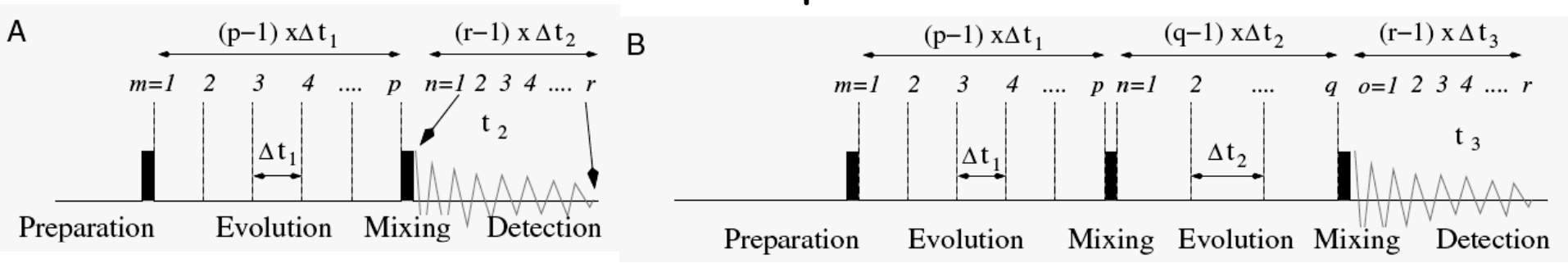

Figure 9.2. Generalized two-dimensional and three-dimensional pulse sequences. Panels A and B show a two-dimensional or a three-dimensional experiment, respectively. Both experiments begin with an excitation pulse that is followed by an evolution period, t_1, and then a mixing period. In a two-dimensional experiment the FID is collected after the mixing period. In the case of a three-dimensional experiment, another evolution and mixing period follow before acquisition of the FID. Initially, the length of the t_1 period is set to zero (or $\Delta t_1/2$) and the first (m = 1) FID containing r points is collected. Note that this FID usually consists of multiple scans, all of which are summed to the same memory location. Subsequently, t_1 is incremented by a fixed amount, Δt_1 (the dwell time in t_1), and a second (m = 2) FID is collected and stored in a different memory location. This process is repeated a total of p times until the desired evolution time is attained. In the case of the three-dimensional experiment (B), the t_1 and t_2 evolution periods are sampled independently. For every t_1 time, q t_2 times would be acquired, leading to a total of p×q separate FIDs. Note that the increment in t_1 (Δt_1) need not equal the increment in t_2 (Δt_2), nor does p necessarily equal q.

Any two-dimensional NMR experiment can be divided into four basic elements: preparation, evolution, mixing, and detection.

1. Preparation period: The length of this period is fixed and is usually employed to allow the spins to return to, or near, thermodynamic equilibrium. This period typically ends with a single 90° pulse that excites the first spin ('A').
2. Evolution period (t_1): This time period is used to encode the chemical shift of 'A' in the density matrix due to evolution under the Hamiltonian: $H = \omega_A I_{AZ}$. This period is referred to as the indirectly detected domain, or dimension, because the excited state of spin 'A' is not directly detected by the receiver coil. Rather, the evolution of the system I is sampled digitally, i.e. t_1 begins at zero and then is incremented by a constant amount, Δt_1, with a separate FID acquired at each increment of t_1. A total of p FIDs are acquired, generating a total acquisition time in t_1 of $(p - 1) \times \Delta t_1$.
3. Mixing period: This event causes the magnetization that is associated with spin 'A' to become associated with spin 'B'. This period leads to the transfer of the chemical shift information of spin 'A' to spin 'B'. The mixing can be evoked by either J-coupling or dipolar coupling. The key point is that the amount of magnetization transferred from A to B is proportional to cos(ωAt1) or $\sin(\omega_A t_1)$. Hence the magnetization of 'B' becomes amplitude modulated by a function that contains information about ω_A.
4. Detection Period: During this period of direct detection, the magnetization that is precessing in the x-y plane is detected in the normal fashion. This signal is also sampled digitally, with a time interval of Δt_2, the usual dwell time, giving a total acquisition time of $(r - 1) \times \Delta t_2$. In a three dimensional experiment, the evolution period and mixing period would be repeated an additional time.

In practice, this transform is computed one dimension at a time, usually beginning with the transform of the data as a function of t2, followed by transformation as a

Figure 9.3 Data structure for two dimensional data. The data structure for a two-dimensional data set is shown. Each row corresponds to a FID of r points that was acquired at the indicated t_1 value. There are a total of p t_1 values. Each FID may result from the sum of more than one scan, but all scans would be acquired with the same t_1 value.

	$t_2 \longrightarrow$									
$t_1 \downarrow$	1	2	3	4	5	6	7	8	.	r
1	x	x	x	x	x	x	x	x	.	.
2	x	x	x	x	x	x	x	x	.	.
3	x	x	x	x	x	x	x	x	.	.
4	x	x	x	x	x	x	x	x	.	.
5	x	x	x	x	x	x	x	x	.	.
.	.	.	.	.	.	.	.	.	.	.
p	.	.	.	.	.	.	.	.	.	.

$$F(t_1, \omega_2) = \int S(t_1, t_2) e^{i\omega t_2} dt_2 \qquad \Omega(\omega_1, \omega_2) = \int F(t_1, \omega_2) e^{i\omega t_1} dt_1$$

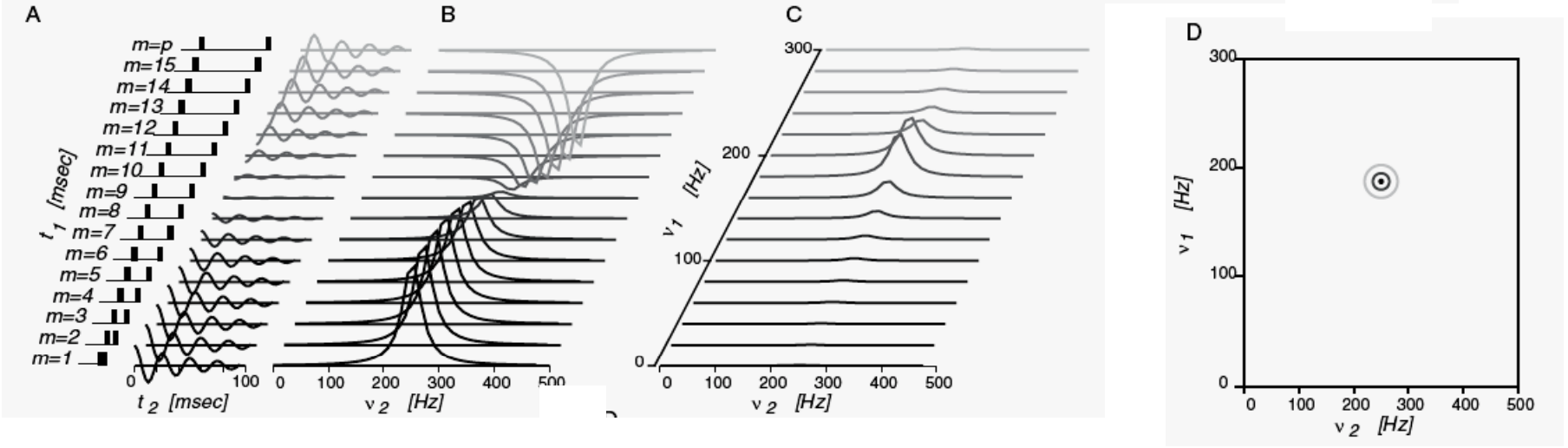

Figure 9.4. Generation of a two-dimensional spectrum. In this example the frequency of the two coupled spins are 190 and 250 Hz. Note that only one magnetization path is considered here (i.e. A → B), therefore only one peak is present in the spectrum, located at ν_A = 190 Hz and ν_B = 250 Hz.

9.2 Homonuclear J-correlated Spectra

In this section we will look with some detail at two common two-dimensional homonuclear J-correlated experiments, the COSY (COrrelated SpectroscopY) and the DQF-COSY (Double-Quantum Filtered COSY). The COSY experiment was first presented by Jeener in 1971 [78] and was given its current name in 1980 [91]. The DQF-COSY experiment is a specific example of a multiple-quantum filtered COSY experiment [131].

9.2.1 COSY Experiment

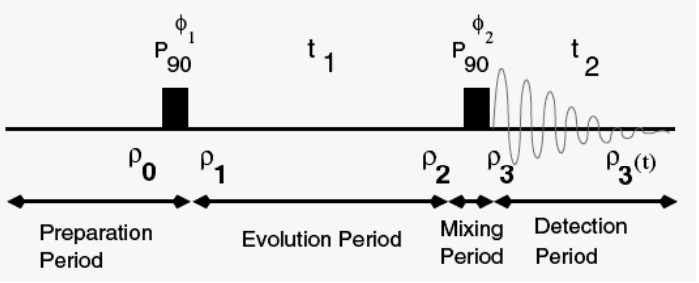


```
  1 ze                  ;Zero the memory.
  2 d1                  ;Inter-scan relaxation delay (1 sec)
  3 (p1 ph1):f1         ;Pulse of length p1, phase=ph1 on channel 1.
    d0                  ;t1 evolution time
    (p1 ph2):f1         ;Second 90 pulse, with phase=ph2 (mixing pulse)
    go=2 ph31           ;Acquire FID (Receiver phase=31) go to 2, n-times
    write               ;Write the FID to disk.
    id0                 ;increment t1 time
    lo to 3 times td1   ;go to 3 p times (total number of t1 values)
  exit                  ;End of pulse sequence.
ph1 =0 0 0 0 1 1 1 1 2 2 2 2 3 3 3 3 ;Phase of 1st excitation pulse.
ph2 =0 1 2 3 0 1 2 3 0 1 2 3 0 1 2 3 ;Phase of 2nd pulse.
ph31=0 2 0 2 3 1 3 1 2 0 2 0 1 3 1 3 ;Phase of receiver.
```

Figure 9.5. COSY pulse sequence. The figure on the left shows the COSY pulse sequence while the right panel shows the corresponding pulse program that is used to represent the sequence. The text to the right of the semi-colon in the pulse program briefly describes each step of program. The COSY experiment consists of two 90° pulses that bracket the t_1 evolution time. The phase of these pulses, as well as the phase of the receiver, are cycled as indicated in the last three lines of the pulse program. A total of p t_1 times are acquired, each of which consisting of n-scans. The second pulse serves to transfer the magnetization from one coupled spin to the other. The density matrices at various points in the pulse sequence are indicated by ρi. The density matrix immediately after the second pulse is ρ_3, which evolves during detection of the FID, giving $\rho_3(t)$.

9.2.1.1 Overall Change of ρ During the COSY Experiment

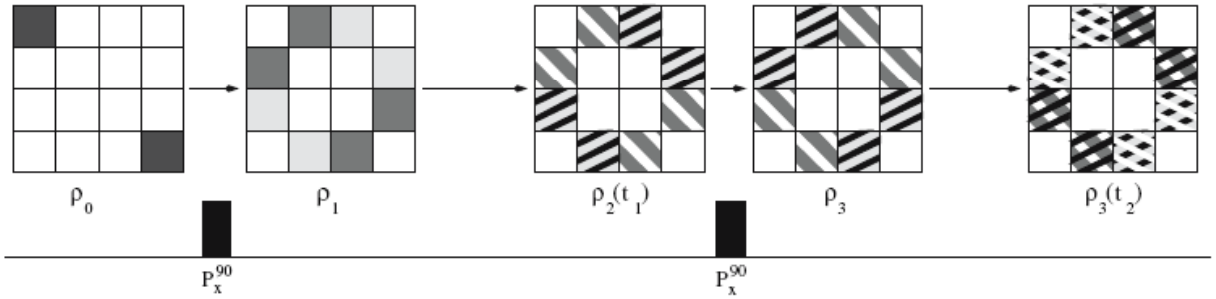

Evolution of the Density Matrix

	$\alpha\alpha$	$\alpha\beta$	$\beta\alpha$	$\beta\beta$
$\alpha\alpha$	P_1	Ω_S	Ω_I	Ω_{IS}
$\alpha\beta$	Ω_S	P_2	Ω_0	Ω_I
$\beta\alpha$	Ω_I	Ω_0	P_3	Ω_S
$\beta\beta$	Ω_{IS}	Ω_I	Ω_S	P_4

Figure 9.6. Pictorial representation of density matrix changes during the COSY experiment. The changes that occur in the density matrix during the COSY experiment are illustrated in this figure. The non-zero elements of the density matrix are shaded. A solid shading indicates that no time evolution has occurred. Squares shaded with a light gray background are initially associated with I spins and squares shaded in darker gray are initially associated with S spins. These associations are interchanged by the mixing pulse. Right-slanted black-lines ( ) indicate evolution of the element of the density matrix at the chemical shift of spin I. Left-slanted white-lines ( ) indicate evolution of the element of the density matrix at the chemical shift of spin S. Double crosshatched squares indicate evolution at ω_I in t_1 and ω_S in t_2 ( ) or at ω_S in t_1 and ω_I in t_2 ( ). The pulse sequence is shown below the 4×4 density matrices. For reference, each element of the density matrix evolves according to the following table shown to the right.

9.2.1.2 Density Matrix/Product Operator Analysis of the COSY Experiment

The initial density matrix of the system is: $\rho_o = I_z + S_z$

The first pulse is a 90° pulse along the x-axis. Since this is a homonuclear experiment this pulse is applied to both spins, bringing the magnetization from the z-axis to the minus y-axis. The transformation of the density matrix is:

$$\rho = e^{-i\beta Ix} e^{-i\beta Sx} \rho_o e^{i\beta Ix} e^{i\beta Sx}$$

$$\rho_1 = e^{-i\beta I_x} I_z e^{i\beta I_x} + e^{-i\beta S_x} S_z e^{i\beta S_x} = I_z cos\beta - I_y sin\beta + S_z cos\beta - S_y sin\beta$$
$$= -[I_y + S_y] \qquad (\beta = 90^\circ)$$

During t_1 the density matrix evolves under the complete Hamiltonian, by applying the following transformation to ρ_1:

$$R = e^{i(\omega_I t_1 I_z + \omega_S t_1 S_z + \pi J 2 I_z S_z t_1)}$$

Since all of these operators commute, they can be considered separately and rearranged for convenience. In this case we will evaluate evolution due to chemical shift of the S spin first, followed by evolution due to the chemical shift of the I spin, followed lastly by J-coupling. This gives the following transformation of the density matrix:

$$\rho_2 = e^{i\pi J 2 I_z S_z t_1} \left[e^{i\omega_I t_1 I_z} \left[e^{i\omega_S t_1 S_z} \rho_1 e^{i\omega_S t_1 S_z} \right] e^{i\omega_I t_1 I_z} \right] e^{i\pi J 2 I_z S_z t_1}$$

During evolution:

$$-I_y \rightarrow -[I_y cos(\omega_I t_1) - I_x sin(\omega_I t_1)] \qquad -S_y \rightarrow -[S_y cos(\omega_S t_1) - S_x sin(\omega_S t_1)]$$

The effect of scalar coupling on each of the terms in the above equation is:

$I_y \rightarrow I_y \cos(\pi J t_1) - 2 I_x S_z \sin(\pi J t_1)$; $\quad Sy \rightarrow S_y \cos(\pi J t_1) - 2 I_z S_x \sin(\pi J t_1)$

$I_x \rightarrow I_x \cos(\pi J t_1) + 2 I_y S_z \sin(\pi J t_1)$; $\quad Sx \rightarrow S_x \cos(\pi J t_1) + 2 I_z S_y \sin(\pi J t_1)$

The combined effect of these two transformations is:

$$\begin{aligned}\rho_2 = \quad & -I_y cos(\omega_I t_1) cos(\pi J t_1) + 2 I_x S_z cos(\omega_I t_1) sin(\pi J t_1) \\ & -S_y cos(\omega_S t_1) cos(\pi J t_1) + 2 I_z S_x cos(\omega_S t_1) sin(\pi J t_1) \\ & +I_x sin(\omega_I t_1) cos(\pi J t_1) + \underline{2 I_y S_z sin(\omega_I t_1) sin(\pi J t_1)} \\ & +S_x sin(\omega_S t_1) cos(\pi J t_1) + \underline{2 I_z S_y sin(\omega_S t_1) sin(\pi J t_1)}\end{aligned}$$

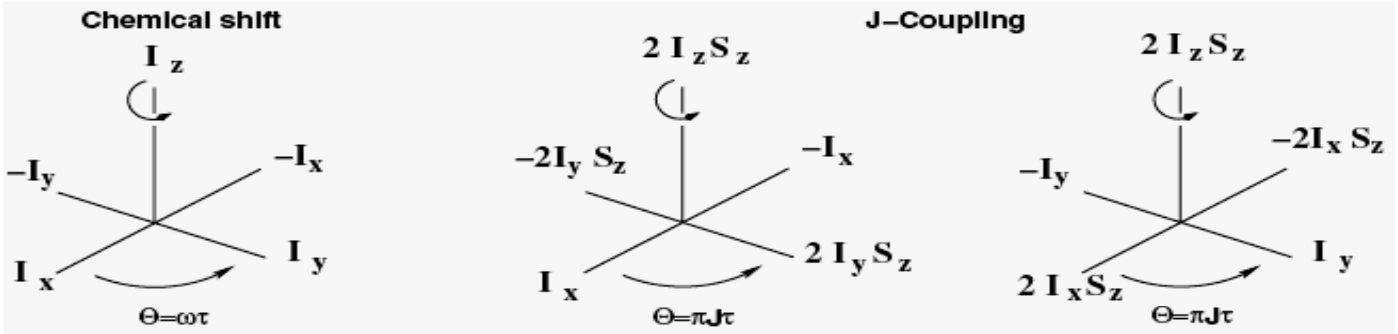

Figure 9.7. Transformation of ρ by chemical shift and J-coupling.

The underlined terms will ultimately produce the crosspeaks in the spectrum, as discussed below. The effect of the second 90◦ x-pulse on the various terms in the above equation is shown to the right of the arrows (the trigonometric terms have been ignored temporarily):

The effect of the second 90◦ x-pulse on the various terms in the above equation is shown to the right of the arrows (the trigonometric terms have been ignored temporarily):

$I_y \rightarrow I_z$; $S_y \rightarrow S_z$; $I_x \rightarrow I_x$; $S_x \rightarrow S_x$;2IxSz →-2IxSy; 2IzSx →-2IyS$_x$

$$\underline{2I_yS_z \rightarrow -2I_zS_y} \quad \underline{2I_zS_y \rightarrow -2I_yS_z}$$

The first line, containing I_z and S_z, corresponds to a density matrix with only diagonal matrix elements, representing undetectable magnetization. Terms in the second line (I_x and S_x) are detectable, but they will only produce diagonal peaks because the same spin is transverse before and after the mixing pulse. Therefore these elements of the density matrix will evolve with the same frequency during t_1 and t_2. The third line contains terms that represent the creation of double quantum coherence after the second pulse. These cannot be detected in the experiment. The last line contains the two terms of interest, those which will generate crosspeaks.

9.2.1.3 Origin of COSY Crosspeaks

The crosspeaks in the COSY spectrum arise from the following product operators:

$$2I_yS_z \overset{90^\circ_x}{\rightarrow} -2I_zS_y \qquad 2I_zS_y \overset{90^\circ_x}{\rightarrow} -2I_yS_z$$

The transformation by the 90◦ pulse causes the transverse magnetization that was associated with one spin to be transferred to the other spin. This can be seen by inspection of the density matrix which corresponds to these product operators, for example:

$$2I_yS_z sin(\omega_I t_1) sin(\pi J t_1) =$$

$$\begin{bmatrix} 0 & 0 & -i\,\Omega_I sin(\pi J t_1) & 0 \\ 0 & 0 & 0 & i\,\Omega_I sin(\pi J t_1) \\ i\,\Omega_I sin(\pi J t_1) & 0 & 0 & 0 \\ 0 & -i\,\Omega_I sin(\pi J t_1) & 0 & 0 \end{bmatrix}$$

Where sin(ω1t1) has been replaced by Ω_1. After the 90° pulse this density matrix becomes:

$$\begin{bmatrix} 0 & -i\,\Omega_I sin(\pi J t_1) & 0 & 0 \\ i\,\Omega_I sin(\pi J t_1) & 0 & 0 & 0 \\ 0 & 0 & 0 & -i\,\Omega_I sin(\pi J t_1) \\ 0 & 0 & i\,\Omega_I sin(\pi J t_1)) & 0 \end{bmatrix}$$

The matrix elements that represent single quantum transitions of one spin, such as $-i\Omega_I sin(\pi J t_1)$, have been moved to elements of the density matrix that evolve with the frequency of the other spin (Ω_S) during t_2.Therefore the amplitude of the density matrix element that evolves at a frequency of ω_S during t_2 is $sin(\omega_I t_1)sin(\pi J t_1)$. The complete expression for the density matrix that describes the crosspeaks is:

$$\rho_3 = -2I_zS_y sin(\omega_I t_1) sin(\pi J t_1) - 2I_yS_z sin(\omega_S t_1) sin(\pi J t_1)$$

$$\frac{1}{2}E = \frac{1}{2}\begin{bmatrix} 1 & 0 & 0 & 0 \\ 0 & 1 & 0 & 0 \\ 0 & 0 & 1 & 0 \\ 0 & 0 & 0 & 1 \end{bmatrix}$$

$$2I_zS_z = \frac{1}{2}\begin{bmatrix} 1 & 0 & 0 & 0 \\ 0 & -1 & 0 & 0 \\ 0 & 0 & -1 & 0 \\ 0 & 0 & 0 & 1 \end{bmatrix}$$

$$I_x = \frac{1}{2}\begin{bmatrix} 0 & 0 & 1 & 0 \\ 0 & 0 & 0 & 1 \\ 1 & 0 & 0 & 0 \\ 0 & 1 & 0 & 0 \end{bmatrix}$$

$$S_x = \frac{1}{2}\begin{bmatrix} 0 & 1 & 0 & 0 \\ 1 & 0 & 0 & 0 \\ 0 & 0 & 0 & 1 \\ 0 & 0 & 1 & 0 \end{bmatrix}$$

$$I_y = \frac{1}{2}\begin{bmatrix} 0 & 0 & -i & 0 \\ 0 & 0 & 0 & -i \\ i & 0 & 0 & 0 \\ 0 & i & 0 & 0 \end{bmatrix}$$

$$S_y = \frac{1}{2}\begin{bmatrix} 0 & -i & 0 & 0 \\ i & 0 & 0 & 0 \\ 0 & 0 & 0 & -i \\ 0 & 0 & i & 0 \end{bmatrix}$$

$$I_z = \frac{1}{2}\begin{bmatrix} 1 & 0 & 0 & 0 \\ 0 & 1 & 0 & 0 \\ 0 & 0 & -1 & 0 \\ 0 & 0 & 0 & -1 \end{bmatrix}$$

$$S_z = \frac{1}{2}\begin{bmatrix} 1 & 0 & 0 & 0 \\ 0 & -1 & 0 & 0 \\ 0 & 0 & 1 & 0 \\ 0 & 0 & 0 & -1 \end{bmatrix}$$

$$2I_xS_x = \frac{1}{2}\begin{bmatrix} 0 & 0 & 0 & 1 \\ 0 & 0 & 1 & 0 \\ 0 & 1 & 0 & 0 \\ 1 & 0 & 0 & 0 \end{bmatrix}$$

$$2I_yS_y = \frac{1}{2}\begin{bmatrix} 0 & 0 & 0 & -1 \\ 0 & 0 & 1 & 0 \\ 0 & 1 & 0 & 0 \\ -1 & 0 & 0 & 0 \end{bmatrix}$$

$$2I_xS_z = \frac{1}{2}\begin{bmatrix} 0 & 0 & 1 & 0 \\ 0 & 0 & 0 & -1 \\ 1 & 0 & 0 & 0 \\ 0 & -1 & 0 & 0 \end{bmatrix}$$

$$2I_yS_z = \frac{1}{2}\begin{bmatrix} 0 & 0 & -i & 0 \\ 0 & 0 & 0 & i \\ i & 0 & 0 & 0 \\ 0 & -i & 0 & 0 \end{bmatrix}$$

$$2I_zS_x = \frac{1}{2}\begin{bmatrix} 0 & 1 & 0 & 0 \\ 1 & 0 & 0 & 0 \\ 0 & 0 & 0 & -1 \\ 0 & 0 & -1 & 0 \end{bmatrix}$$

$$2I_xS_y = \frac{1}{2}\begin{bmatrix} 0 & 0 & 0 & -i \\ 0 & 0 & i & 0 \\ 0 & -i & 0 & 0 \\ i & 0 & 0 & 0 \end{bmatrix}$$

$$2I_zS_y = \frac{1}{2}\begin{bmatrix} 0 & -i & 0 & 0 \\ i & 0 & 0 & 0 \\ 0 & 0 & 0 & i \\ 0 & 0 & -i & 0 \end{bmatrix}$$

$$2I_yS_x = \frac{1}{2}\begin{bmatrix} 0 & 0 & 0 & -i \\ 0 & 0 & -i & 0 \\ 0 & i & 0 & 0 \\ i & 0 & 0 & 0 \end{bmatrix}$$

These product operators are not directly detectable, however they evolve into detectable magnetization due to the J-coupling term in the Hamiltonian. Temporarily neglecting amplitude factors (e.g. $\sin(\omega_I t_1)\sin(\pi J t_1)$), the evolution of these product operators are:

$$\rho_3 \xrightarrow{J} \rho_3'$$

$$-2I_zS_y \rightarrow -2I_zS_y cos(\pi J t_2) + S_x sin(\pi J t_2)$$

$$-2I_yS_z \rightarrow -2I_yS_z cos(\pi J t_2) + I_x sin(\pi J t_2)$$

Forming I^- and S^-, and incorporating the amplitude factors from evolution in t_1 as well as evolution due to J-coupling in t_2, gives the following for the detectable portion of the density matrix:

$$\rho_3(t) = I^-[sin(\omega_s t_1)sin(\pi J t_1)sin(\pi J t_2)e^{i\omega_I t_2}] + S^-[(sin(\omega_I t_1)sin(\pi J t_1)sin(\pi J t_2)e^{i\omega_S t_2}]$$

The detected signal is obtained by evaluating Trace[$\rho(I^+ + S^+)$]:

$$S(t_1,t_2) = sin(\omega_S t_1)sin(\pi J t_1)sin(\pi J t_2)e^{i\omega_I t_2} + sin(\omega_I t_1)sin(\pi J t_1)sin(\pi J t_2)e^{i\omega_S t_2}$$

9.2.1.4 Origin of COSY Diagonal Peaks

The diagonal peaks in the COSY spectrum arise from the I_x and S_x terms that are present after the second 90° pulse. Choosing to focus on the I spin only, and temporarily ignoring amplitude factors from evolution during t1, the evolution under J-coupling is:

$$I_x \xrightarrow{J} I_x cos(\pi J t_2) + I_y S_z sin(\pi J t_2)$$

Only the I_x term will be detectable, thus its evolution under chemical shift is:

$$I_x \xrightarrow{\Omega} I_x cos(\omega_I t_2) + I_y sin(\omega_I t_2)$$

Incorporating the amplitude factors associated with I_x from evolution during t_1 give the following:

$\rho_3(t) = I_x \sin(\omega_I t_1)\cos(\pi J t_1)\cos(\pi J t_2)\cos(\omega_I t_2) + I_y \sin(\omega_I t_1)\cos(\pi J t_1)\cos(\pi J t_2)\sin(\omega_I t_2)$

Substituting $I_x = 1/2\ [I^+ + I^-]$ and $I_y = 1/2i\ [I^+ - I^-]$ gives the amplitude of the I^- part of the density matrix:

$$\rho_3(t) = I^-[sin(\omega_I t_1)cos(\pi J t_1)cos(\pi J t_1)e^{i\omega_I t_2}]$$

Therefore the signal that is associated with the diagonal peak is:

$$S(t_1, t_2) = sin(\omega_I t_1)cos(\pi J t_1)cos(\pi J t_1)e^{i\omega_I t_2}$$

9.2.1.5 Appearance of the COSY Spectrum

The signal that gives rise to the crosspeaks is:

$$S(t_1, t_2) = sin(\omega_S t_1)sin(\pi J t_1)sin(\pi J t_2)e^{i\omega_I t_2} + sin(\omega_I t_1)sin(\pi J t_1)sin(\pi J t_2)e^{i\omega_S t_2} \quad (9.28)$$

while the signal that is associated with the diagonal peaks is:

$$S(t_1, t_2) = sin(\omega_I t_1)cos(\pi J t_1)cos(\pi J t_1)e^{i\omega_I t_2} + sin(\omega_S t_1)cos(\pi J t_1)cos(\pi J t_1)e^{i\omega_S t_2} \quad (9.29)$$

The position of these peaks in the 2D-spectrum is determined by the terms that contain chemical shift information. For example, $\sin(\omega_S t_1)e^{i\omega_I t_2}$ specifies a crosspeak at (ω_S, ω_I). Therefore, Eq. 9.28 represents the two crosspeaks and Eq. 9.29 represents the two diagonal peaks, at (ω_I, ω_I) and (ω_S, ω_S), as expected.

The additional terms in eqs. 9.28 and 9.29, such as $\sin(\pi J t_1)$, are responsible for generating the splitting of each peak by the J-coupling. Since the time domain signal is a product of two functions in each dimension, its Fourier transform will be the convolution of the individual transforms with each other. For example,

$$sin(\pi J t)e^{i\omega t} \overset{FT}{\rightarrow} FT\left[(sin(\pi J t))\right] \otimes FT\left[(e^{i\omega t})\right]$$

In the case of the crosspeak, the resonance peak is convoluted with the Fourier transform of sin(πJt). This produces an anti-phase doublet, with a negative peak at −πJ and a positive peak at +πJ. Note that the overall splitting between these two peaks is 2π J rad/sec (or J Hz), as expected. Note that this splitting occurs in both dimensions, thus forming a quartet of peaks. In addition to the introduction of the antiphase splitting of the line, the convolution with the Fourier transform of sin(πJt) also causes the spectrum to be complex, since the transform of sine is imaginary. Therefore, the crosspeaks will have a dispersion lineshape.

The diagonal peaks are modulated by cos(πJt), whose transform is doublet of real and positive peaks at ±πJ. Convolution of this function with $e^{i\omega t2}$ will give an in-phase (i.e. both positive) doublet that will have an absorption mode lineshape. Again, this splitting occurs in both dimensions, leading to a quartet of peaks with an absorption lineshape.

Since the crosspeaks are usually of interest, they are phased to generate absorption lineshapes. Clearly, the same phase correction has to be applied to the diagonal peaks as well. Consequently, the diagonal peaks will be 90° out-of-phase and will have a dispersion lineshape, as indicated in Fig. 9.9.

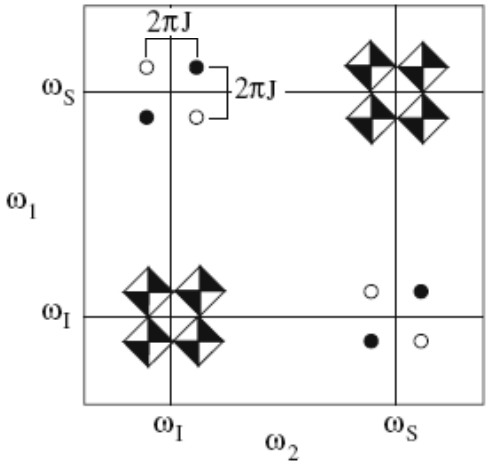

Figure 9.8 Sketch of an AX COSY spectrum. A schematic diagram of a COSY spectrum is shown for two coupled spins, I and S. The circles represent peaks with an absorption mode lineshape. Filled circles are positive and empty circles are negative. The spectrum has been phased such that the crosspeaks are absorption mode, thus the diagonal peaks have a dispersion lineshape in both dimensions, which is represented by the symbol ..

Figure 9.9. Lineshape in the COSY spectrum. A more detailed view of lower half of the COSY spectrum that was shown in Fig. 9.8 is presented here. Note that the diagonal peak (left) is a dispersion lineshape, while the crosspeaks have an absorption lineshape.

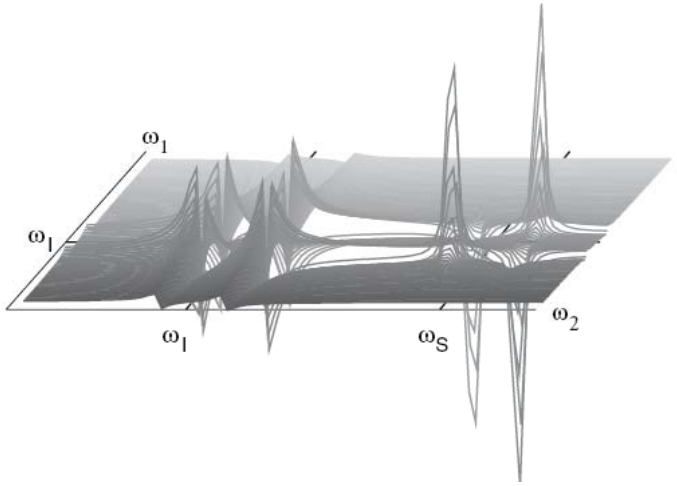

9.3 Double Quantum Filtered COSY (DQF-COSY)

The COSY experiment has several drawbacks, even though it is one of simplest two-dimensional experiments. First, the dispersive nature of the diagonal selfpeaks can cause considerable distortion of crosspeaks that are found near the diagonal of the spectrum. Second, the solvent peak (e.g. water), is not suppressed in the experiment. In the case of protein spectra acquired in H_20, the solvent peak can be several orders of magnitude larger than the protein resonances, causing a considerable dynamic range problem.

The double quantum filtered COSY experiment, or DQF-COSY, does not suffer from these deficiencies. This experiment filters out any signals that do not arise from coupled spins. Since the protons in water are equivalent, they behave as if they are not coupled and will be absent from the DQF-COSY spectrum. An additional benefit of the DQF-COSY experiment is that both the diagonal and the crosspeaks can be phased to be in pure absorption mode, producing a much cleaner spectrum in the diagonal region.

The DQF-COSY experiment is shown in Fig. 9.10. It is very similar to the COSY sequence, with the exception that the single mixing pulse in the COSY experiment has been replaced by two 90◦ pulses in the DQF-COSY. The first of these pulses converts the single quantum states to double quantum states. The last pulse returns this double quantum magnetization to detectable single quantum magnetization. The
experiment filters out any elements of the density matrix that does not pass though a double quantum state. This filtering occurs as a result of the phase cycle. A more detailed analysis will be presented in Chapter 11. For the meantime we will assume that it occurs. The overall evolution of the elements of the density matrix are illustrated in Fig. 9.11.

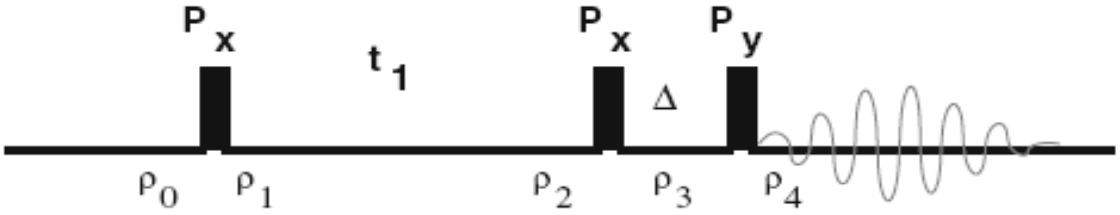

Figure 9.10. Double quantum filtered COSY (DQF-COSY) pulse sequence. All pulses are 90° pulses. The delay Δ is just long enough to change the phase of the transmitter, or about 10 μsec. Consequently evolution of the density matrix during this period can be ignored. The detected signal is given by Trace$[\rho_4(t)I^+]$.

9.3.1 Product Operator Treatment of the DQF-COSY Experiment

To simplify the analysis we will focus on just the I spins at the beginning of the experiment. Due to symmetry, the evolution of the S spins can be easily calculated by interchanging I and S in the following derivation. Setting $\rho_0 = I_z$ gives the following:

$$\rho_2 = -I_y cos(\omega_I t_1) cos(\pi J t_1) + 2I_x S_z cos(\omega_I t_1) sin(\pi J t_1) + I_x sin(\omega_I t_1) cos(\pi J t_1) + 2I_y S_z sin(\omega_I t_1) sin(\pi J t_1)$$

$-I_y \rightarrow -I_z$; $I_x \rightarrow I_x$; $2I_xS_z \rightarrow -2I_xS_y$; $2I_yS_z \rightarrow -2I_zS_y$

In the COSY experiment, it was the last of the above terms, $-2I_zS_y$, that gave rise to the crosspeak. In the DQF-COSY experiment, the only term that survives the double-quantum filter is the $2I_xS_y$. This particular density matrix actually contains both double-quantum and zero-quantum elements:

$$2I_xS_y = \frac{1}{2}\begin{bmatrix} 0 & 0 & 0 & -1 \\ 0 & 0 & 1 & 0 \\ 0 & 1 & 0 & 0 \\ -1 & 0 & 0 & 0 \end{bmatrix}$$

The removal of the zero-quantum terms can be accomplished by writing the above density matrix in terms of the raising and lowering operators:

$$2I_xS_y = 2\frac{1}{2}(I^+ + I^-)\frac{1}{2i}(S^+ - S^-) = \frac{1}{2i}[I^+S^+ - I^+S^- + I^-S^+ - I^-S^-]$$

The density matrices I+S+ and I−S− are non-zero for only elements that represent double-quantum transitions while the matrices I+S− and I−S+ have only nonzero elements that represent zero-quantum transitions. Consequently, after the double quantum filtering has occurred, the density matrix contains only the double-quantum terms:

$$\rho_{3f} = \frac{1}{2i}[I^+S^+ - I^-S^-] = \frac{1}{2i}[(I_x + iI_y)(S_x + iS_y) - (I_x - iI_y)(S_x - iS_y)]$$
$$= \frac{1}{4}[2I_xS_y + 2I_yS_x]$$

The last pulse, P_y^{90}, transforms ρ_{3f} to $\rho(4)$: $[2I_xS_y + 2I_yS_x] \overset{P_y^{90}}{\rightarrow} -[2I_zS_y + 2I_yS_z]$

During detection, these terms evolve due to J-coupling to give detectable singlequantum states:

$$2I_zS_y \overset{J}{\rightarrow} 2I_zS_y cos(\pi Jt_2) - S_x sin(\pi Jt_2) \qquad 2I_yS_z \overset{J}{\rightarrow} 2I_yS_z cos(\pi Jt_2) - I_x sin(\pi Jt_2)$$

The detectable single operator terms evolve with their respective chemical shifts:

$$-S_x \overset{\omega_S}{\rightarrow} -S_x cos(\omega_S t_2) - S_y sin(\omega_S t_2)$$

$$-I_x \overset{\omega_I}{\rightarrow} -I_x cos(\omega_I t_2) - I_y sin(\omega_I t_2)$$

If we include the amplitude factor that was generated during the t_1 evolution time, as well as the trigonometric terms from above, then the final signal is:

$$\begin{aligned} S(t_1, t_2) &= cos(\omega_I t_1) sin(\pi J t_1) sin(\pi J t_2) e^{i\omega_S t_2} \\ &+ cos(\omega_I t_1) sin(\pi J t_1) sin(\pi J t_2) e^{i\omega_I t_2} \end{aligned}$$

The first of these two terms represents the crosspeak at (ω_I, ω_S) and the second represents the selfpeak at (ω_I, ω_I). The spectrum will also contain another crosspeak, at (ω_S, ω_I), and selfpeak, at (ω_S, ω_S), which would be generated if the analysis was started with ρo = Sz instead of Iz.

Note that both the crosspeak and the selfpeak have exactly the same evolution due to J-coupling, specifically $\sin(\pi J t_1)\sin(\pi J t_2)$. Consequently, the selfpeak and the crosspeak will be found as anti-phase doublets that can both be phased to give pure absorption lineshapes. This feature leads to a remarkable improvement in the appearance of the DQF-COSY spectrum over that of the COSY spectrum, especially near the diagonal (see Fig. 9.12).

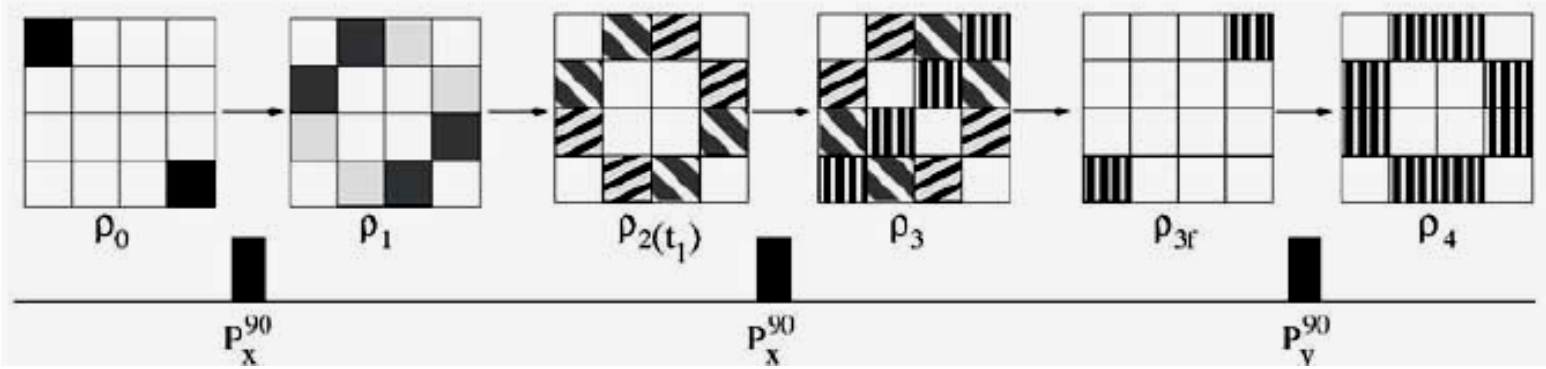

Figure 9.11. **The density matrix during a DQF-COSY experiment.** The density matrix just before the second pulse is identical to that in the COSY experiment. The second pulse generates double and zero quantum states, as indicated by the symbol (▮▮▮). These states also exist in the COSY experiment, but were not detectable. The next density matrix, ρ_{3f} is the filtered density matrix with non-zero values for only the double quantum elements of the density matrix. These elements are converted to detectable single quantum states by the last pulse. **The filtering is accomplished by either phase cycling or pulsed field gradients.**

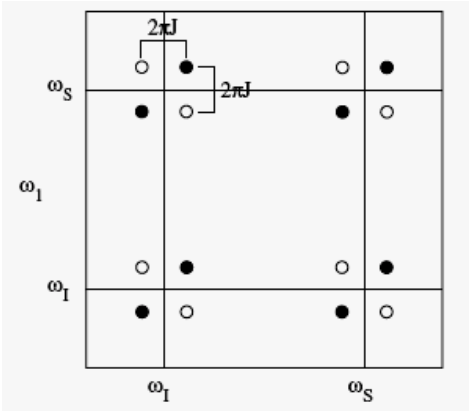

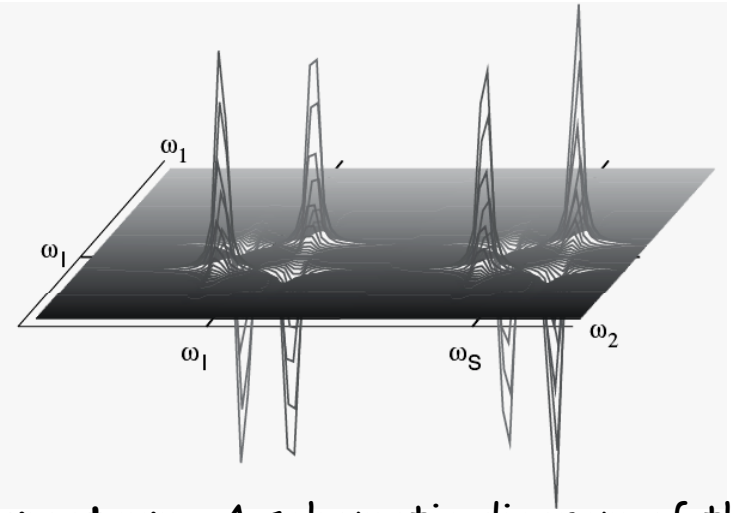

Figure 9.12 Double quantum filtered COSY spectrum. A schematic diagram of the DQF-COSY spectrum is shown. All peaks are pure absorption lineshapes, as illustrated by the spectrum shown in the lower half of the figure.

9.4 Effect of Passive Coupling on COSY Crosspeaks

The previous discussion has focused on the two coupled spins, which define the location of the crosspeak in the COSY or DQF-COSY spectrum. Because these two protons define the location of the crosspeak, they are considered to be actively coupled. The coupling of the active protons to other protons is described as passive coupling. Passive coupling results in additional splitting of the anti-phase quartet. The origin of this additional splitting can be easily seen by analyzing the influence of the passively coupled spin on the evolution of the density matrix during t_1 or t_2. To simplify the analysis, the density matrix associated with the COSY experiment will be used. The same result is obtained for the DQF-COSY experiment.

As an example, consider the effect of passive $J_{\alpha\beta}$ coupling on the crosspeak that is generated from active coupling between an amide proton (S) and an alpha proton (I). During t_1, the two components of the density matrix that ultimately give rise to the crosspeaks are: $2I_zS_y$ and $2I_yS_z$

If the alpha proton is taken to be the I spin, then the term $2I_zS_y$ does not evolve due to the coupling to the H_β protons because the magnetization associated with the a proton is along the z-axis $(\text{i.e. } I_z \overset{J\alpha\beta}{\rightarrow} I_z).$

In contrast, the $2I_yS_z$ term does evolve due to the H_α-H_β coupling because the H_α spin is transverse. The evolution of this part of the density matrix under the passive α-β coupling is as follows:

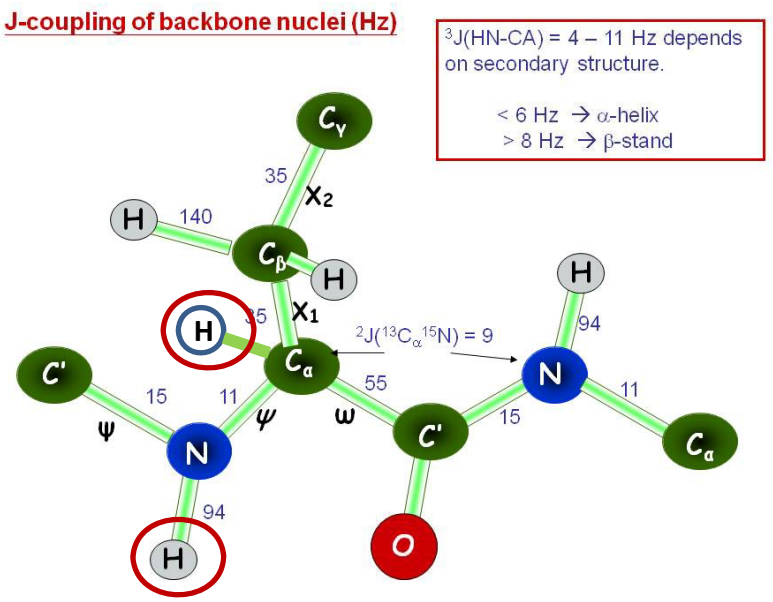

$$\begin{aligned}\rho' &= e^{+i\pi J_{\alpha\beta} I_z K_z} 2I_y S_z e^{-i\pi J_{\alpha\beta} I_z K_z} \\ &= 2S_z e^{+i\pi J_{\alpha\beta} I_z K_z} I_y e^{-i\pi J_{\alpha\beta} I_z K_z} \\ &= 2S_z [I_y cos(\pi J_{\alpha\beta} t_1) - I_x K_z sin(\pi J_{\alpha\beta} t_1)]\end{aligned}$$

where K represents the H_β proton. Only the $2S_zI_y$ part of this density matrix will be detectable, therefore the second term ($2S_zI_xK_z$) can be ignored. Combining evolution due to active coupling and chemical shift gives the following for the final detected signal of the crosspeak that originated with $\rho = 2I_yS_z$:

$$S(t_1, t_2) = cos(\pi J_{\alpha\beta} t_1) sin(\pi J_{\alpha H_N} t_1) sin(\omega_I t_1) sin(\pi J_{\alpha H_N} t_2) e^{i\omega_S t_2}$$

and for the other crosspeak that originated from $\rho = 2I_zS_y$:

$$S(t_1, t_2) = sin(\pi J_{\alpha H_N} t_1) sin(\omega_S t_1) cos(\pi J_{\alpha\beta} t_2) sin(\pi J_{\alpha H_N} t_2) e^{i\omega_I t_2}$$

Note the association of the $\cos(\pi J_{\alpha\beta} t)$ term with the chemical shift evolution of the I proton in both time domain signals. The Fourier transform of this function generates an in-phase doublet, separated by $J_{\alpha\beta}$ Hz, causing an additional splitting of the COSY crosspeak at the Ha frequency, as shown in Fig. 9.13. Normally the passive coupling is smaller than the active coupling. However, the passive coupling between the two alpha protons on glycine is often larger than the active coupling to the amide proton. Consequently, the COSY crosspeaks alternate in intensity, as shown in part C of Fig. 9.13. This feature provides a useful way of identifying glycine residues in COSY spectra.

Passive coupling is also observed when a proton is coupled to two or more equivalent protons. In this case the coupling to one of the equivalent protons is considered to be the active coupling, generating the anti-phase quartet crosspeak, and the coupling to the other proton(s) is considered to be passive, generating additional in-phase splittings. This situation leads to a distinctive pattern of uniform peak spacings for coupling to equivalent CH2 and CH3 groups, as shown in Fig. 9.14. The appearance of the crosspeak in the latter case provides a way of identifying resonance associated with methyl groups in COSY spectra.

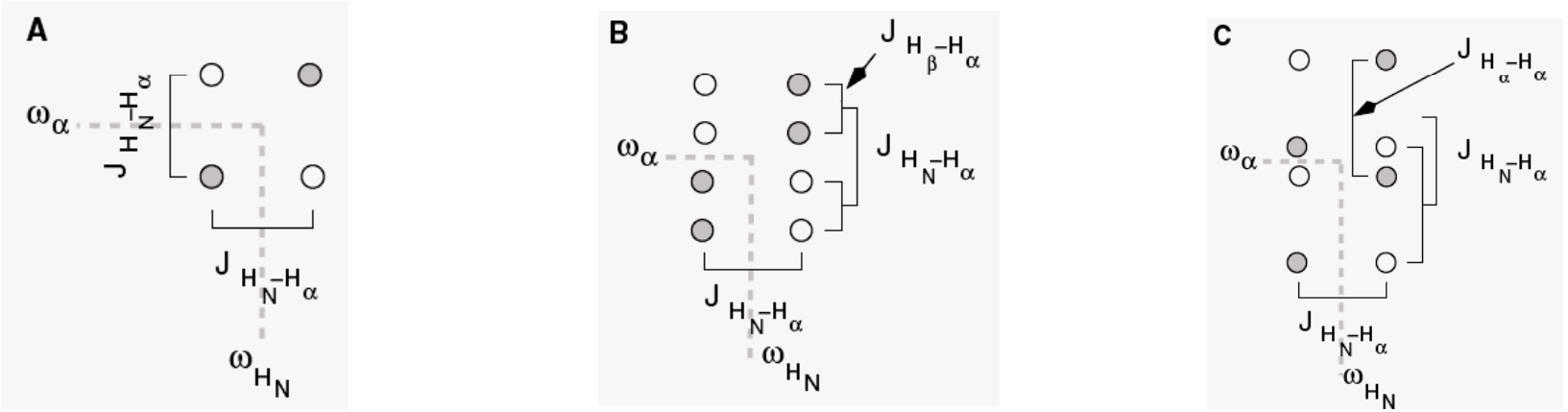

Figure 9.13 Effect of passive coupling on H_N-H_α COSY peaks. A shows the anti-phase quartet located at ω_α and ω_{NH}. The active coupling between the H_α proton and the H_β proton. Note the in-phase splitting of the peaks in these two protons is 9 Hz. B illustrates the effect of a 4 Hz passive coupling between the H_α proton and the H_β proton. Note the in-phase splitting of the peaks in the ω_α dimension. There is no splitting in the H_N dimension because the amide proton is not passively coupled to any protons. C shows the effect of a large passive coupling on the appearance of the cross peak. This often occurs in glycine residues where the passive coupling between the two geminal H_α proton (≈ 15 Hz) exceeds the active coupling between the amide and H_α proton. The effect of the passive coupling between the amide proton and the other H_α proton on the crosspeak pattern is not shown.

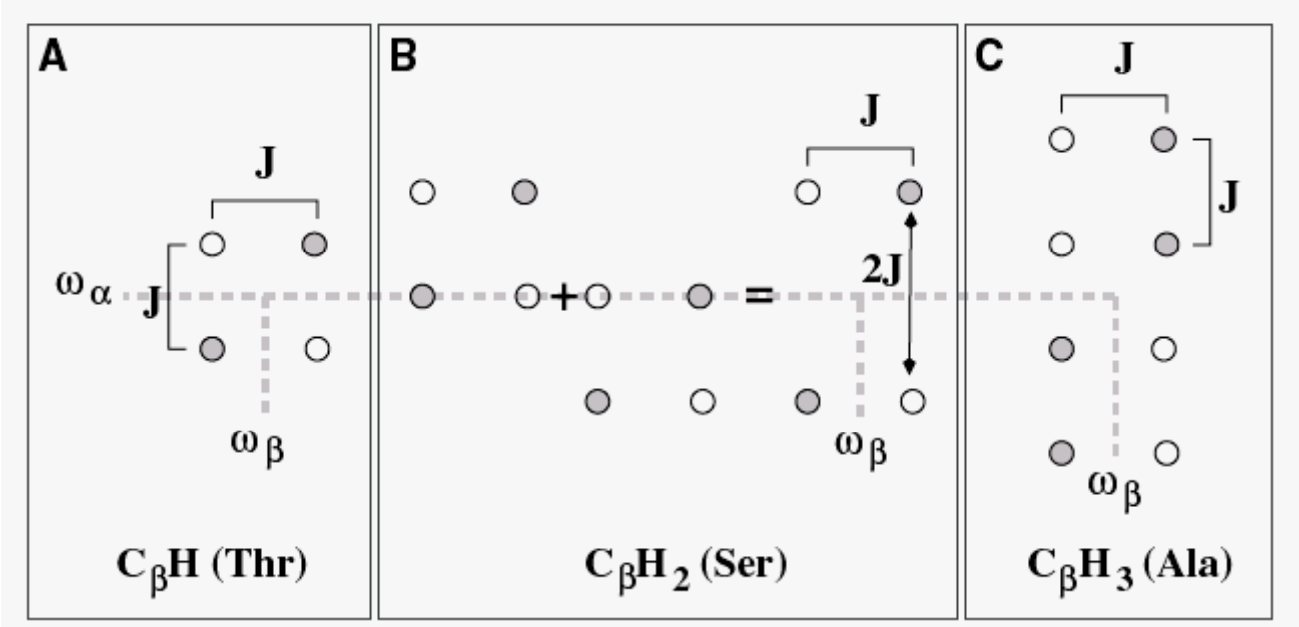

Figure 9.14. *COSY* crosspeaks of CH_2 and CH_3 groups. The *COSY* crosspeak for a proton coupled to one (*A*), two (B) or three (*C*) equivalent protons. If the two actively coupled protons are the α and β protons, then panel *A* corresponds to a threonine residue, panel B to a serine residue, and panel *C* to an alanine residue. In the case of coupling to two equivalent protons (panel B), the in-phase splitting generates two anti-phase doublets that overlap. Consequently, the observed spectrum is the sum of these two. In the left section of this panel the two separate anti-phase quartets have been displaced horizontally to show this cancellation. In the case of coupling to a CH_3 group (panel *C*), the third proton induces an additional in-phase splitting, generating an octet of peaks with equal spacing.

9.5 Scalar Correlation by Isotropic Mixing: TOCSY

In the case of smaller proteins (< 8 kDa), the COSY experiment can be used to identify the complete network of coupled protons within an amino acid residue by the detection of pair-wise interactions. However, as the protein size increases the region of the spectrum that contains correlations between side-chain protons is often quite crowded, making it difficult to identify all of the coupled protons. In addition, the anti-phase nature of the crosspeaks leads to a reduction in the signal-to-noise since the individual anti-phase peaks within the COSY crosspeak destructively interfere with each other. This problem becomes more severe as the size of the protein increases due to an increase in linewidth, as illustrated in Fig. 9.15. For small couplings, such as the HN-Ha coupling in a-helices, it may be difficult to observe crosspeaks in COSY experiments when the molecular weight of the protein exceeds 10 kDa.

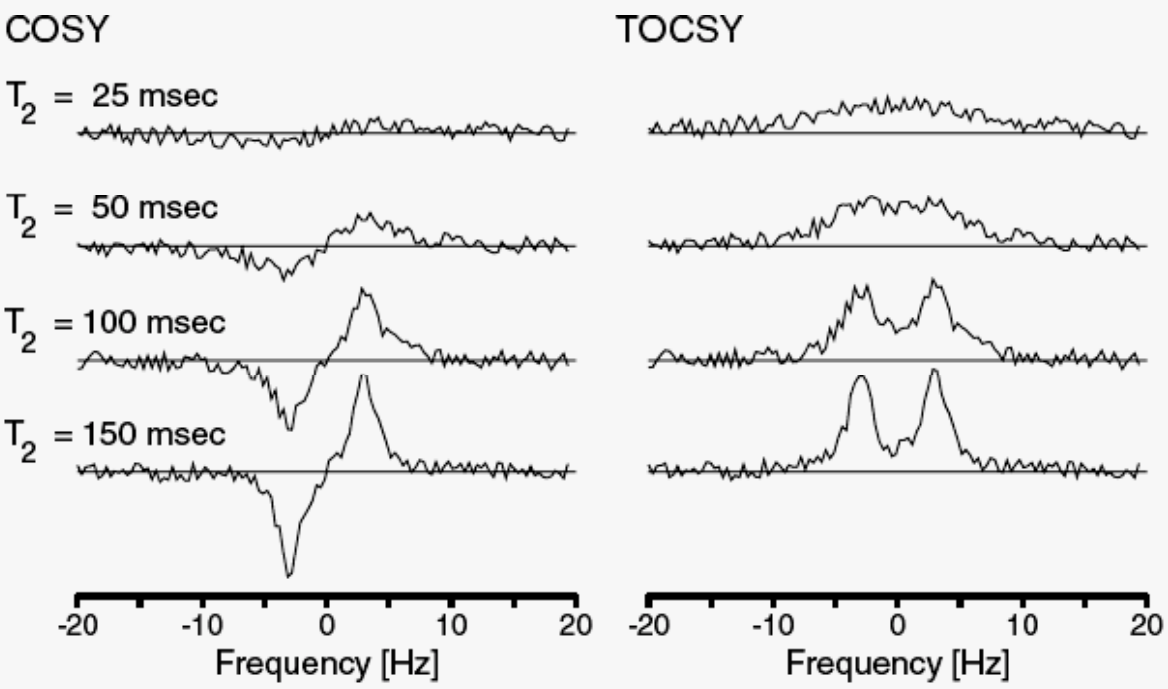

Figure 9.15 COSY versus TOCSY Lineshapes. A cross-section through an anti-phase (COSY) and an in-phase (TOCSY) doublet is shown for a J-coupling of 7 Hz. The lines broaden as the spin-spin relaxation time (T_2) decreases. The lowest curve corresponds to a ≈8 kDa protein while the highest curve corresponds to a ≈50 kDa protein.

The TOCSY, or **TOtal Correlation SpectroscopY, introduced by Braunschweiler** and Ernst [24], solves both of the deficiencies associated with COSY spectra. First, the crosspeaks are composed of lines that are all positive absorption mode, thus preventing the loss of signal via destructive interference (see Fig. 9.15). Second, the chemical shift information of one proton within a spin-system is relayed to all other protons within the spin system. This relay occurs by the sequential transfer of magnetization through the coupled network of spins. For example, a TOCSY peak between the H_N and H_β spin would occur via a two step process. The magnetization that is labeled with the chemical shift of the amide proton would first be passed to the Hα proton via $J_{HNH\alpha}$ coupling, and then to the Hβ proton via $J_{H\alpha H\beta}$ coupling. During t_2, this magnetization would precess at the chemical shift of the H_β proton, generating a crosspeak at (ω_{HN}, $\omega_{H\beta}$). Consequently, crosspeaks associated with the side-chain protons are moved into the relatively sparse amide region of the proton spectrum where individual resonances can be more readily identified.

The TOCSY experiment can also be applied to other spins besides protons. For example, it is possible to exchange magnetization between coupled carbon spins using this technique. Carbon TOCSY experiments play an important role in obtaining chemical shift assignments of sidechain carbons and protons. In the following sections we will investigate the transfer process with little emphasis on the implementation of actual pulse sequences until Chapter 13.

9.5.1 Analysis of TOCSY Pulse Sequence

A simple version of the TOCSY pulse sequence is shown in Fig. 9.16. This pulse sequence consist of an initial 90° pulse, a frequency labeling time (t1), followed by a long series of 180° pulses that are applied to all of the coupled spins1. The 180° pulses prevent evolution of the magnetization by chemical shift during the mixing time. Consequently, the system only evolves under J-coupling during this period, causing transfer of magnetization between coupled spins. (Chemical shift refocused but not J coupling)

Figure 9.16 TOCSY pulse sequence.

The TOCSY pulse sequence is shown in the top of the diagram. Like all other two-dimensional sequences it contains a preparation, t_1 frequency labeling, mixing, and t_2 detection periods. The length of the mixing period is τ and is illustrated here as a train of 180° pulses. In practice it is a series of phase alternated pulses whose net effect is a rotation of the magnetization by 180°. The lower half of the diagram illustrates the fact that each 180° pulse refocuses chemical shift evolution, removing this term from the Hamiltonian.

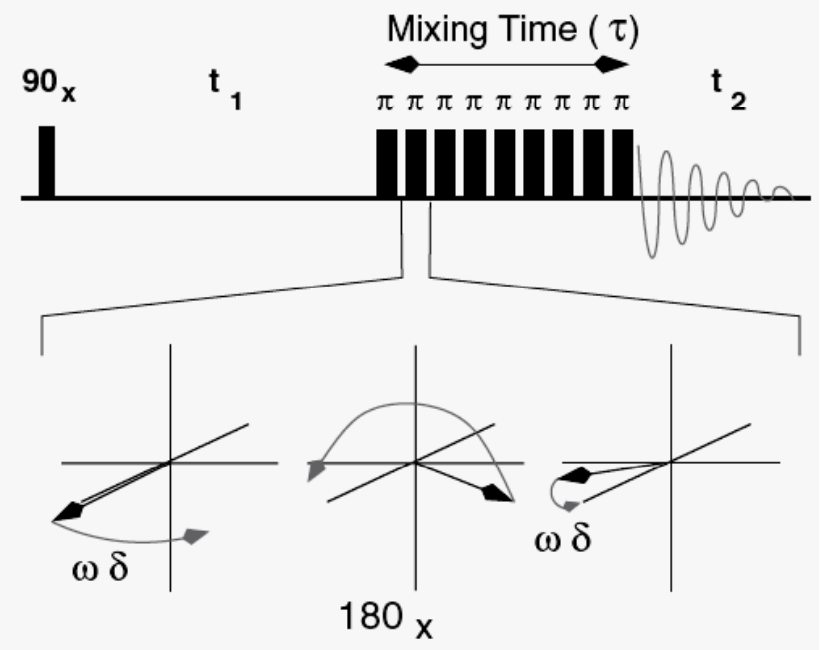

The suppression of chemical shift evolution during the mixing period is accomplished by a spin-echo sequence: *δ–180°–δ.*

$$e^{i0} \xrightarrow{\delta} e^{+i\omega_o\delta} \xrightarrow{180^\circ} e^{-i\omega_o\delta} \xrightarrow{\delta} e^{-i\omega_o\delta} e^{+i\omega_o\delta} = 1$$

The lack of precession due to chemical shift implies that the term of the Hamiltonian that drives chemical shift evolution is effectively zero during the mixing time. Therefore, the only remaining term in the Hamiltonian is the scalar coupling between spins:

$$H = 2\pi J \mathbf{I} \cdot \mathbf{S} = 2\pi J[I_x S_x + I_y S_y + I_z S_z]$$

The term IxSx and IySy must be kept now since the chemical shift is not evolved (i.e. as if Zeeman interaction not present), thus the name "isotropic mixing".

To describe the evolution of the system under the effective Hamiltonian it is necessary to develop new eigenvectors and the associated description of the density matrix.

$$\sum_{\alpha} = \frac{1}{2}[I_\alpha + S_\alpha] \qquad \Delta_\alpha = \frac{1}{2}[I_\alpha - S_\alpha] \qquad \sum_{\alpha\beta} = [I_\alpha S_\beta + I_\beta S_\alpha] \qquad \Delta_{\alpha\beta} = [I_\alpha S_\beta - I_\beta S_\alpha]$$

where $\alpha, \beta, \gamma = x,\ y,\ z,$ e.g. $\Delta_{xy} = [I_x S_y - I_y S_x]$.

The evolution of Δ_α under J-coupling is as follows:

$$\Delta_\alpha \rightarrow \Delta_\alpha cos(2\pi J\tau) + \Delta_{\beta\gamma} sin(2\pi J\tau)$$

where τ is the entire mixing period. In contrast, neither $\sum_\alpha$ or $\sum_{\alpha\beta}$ evolve under J-coupling. **(Verify this ?)**

9.5.1.1 Evolution of Magnetization

At the end of the t1 period the density matrix associated with spin I can be represented, using Cartesian product operators, as:

$$I_x \sin(\omega_1 t_1)\cos(\pi J t_1)$$

I_x can be converted to the new Δ, Σ representation as follows:

$$\sum_x + \Delta_x \rightarrow \sum_x + \Delta_x cos(2\pi J\tau) + \Delta_{yz} sin(2\pi J\tau)$$

The evolution of Ix during the mixing time, τ , is given by:

$$\sum_x +\Delta_x \rightarrow \sum_x +\Delta_x cos(2\pi J\tau) + \Delta_{yz} sin(2\pi J\tau)$$

Converting this expression back to the Cartesian form at the end of the mixing period gives:

$$\begin{aligned} I_x &= \frac{1}{2} I_x \left[1 + cos(2\pi J\tau)\right] + \frac{1}{2} S_x \left[1 - cos(2\pi J\tau)\right] + (I_y S_z - I_z S_y) sin(2\pi J\tau) \\ &= I_x cos^2(\pi J\tau) + S_x sin^2(\pi J\tau) + (I_y S_z - I_z S_y) sin(2\pi J\tau) \end{aligned}$$

The above shows that during the mixing time, magnetization has been transferred from one spin (I_x) to the other coupled spin (S_x). The transfer is weighted by the original amplitude factor of I_x (Eq. 9.50): $[\sin(\omega_1 t_1)\cos(\pi J t_1)]$

So the density matrix of the second spin, after the mixing time, is represented by:

$$S_x[\sin(\omega_I\, t_1)\, \cos(\pi J t_1)]\sin^2(\pi J\tau)$$

where the set of terms in square brackets represent the original amplitude modulation of the I_x term and **the $\sin^2(\pi J\tau)$ represents the magnetization transfered during the mixing time.**

S_x will evolve under chemical shift and J coupling to give as a final detected signal:

$$S(t_1, t_2) = sin^2(2\pi J\tau)[sin(\omega_I t_1)cos(\pi J t_1)]cos(\pi J t_2)e^{i\omega_S t_2}$$

Fourier transformation of this signal will give a crosspeak at (ω_I, ω_S). Note that in contrast to the COSY experiment, the J-coupling term now appears as cos(2πJt) in both time dimensions. Since the Fourier transform of cosine gives a pair of positive peaks, the entire TOCSY crosspeak is positive, as indicated in Fig. 9.15.

The above analysis demonstrates transfer of magnetization from the x-component of spin I to the x-component of spin S. However, by simply changing the indices (e.g. replace x with y) it should be clear that exactly the same transfer would occur between the y- or z-components of the magnetization. This behavior is predicted from the effective Hamiltonian, which has no preferred direction. Consequently, the pulse train in the mixing time is usually referred to as an *isotropic mixing sequence* because it is capable of transferring magnetization along any axis. For example, the sequence shown in Fig. 9.17 would generate crosspeaks by causing transfer of magnetization from I_z to S_z during the mixing time.

9.5.2 Isotropic Mixing Schemes

Efficient isotropic mixing requires that the pulse sequence used to generate the effective Hamiltonian ($2\pi J\mathbf{I}\cdot\mathbf{S}$) is independent of the chemical shifts of the coupled spins. Since the series of π pulses used in Fig. 9.16 can also behave as decoupling sequences, it is not surprising then that the decoupling schemes discussed in Section 7.4 also function as isotropic mixing sequences with the same relative efficiency and bandwidth. For proton isotropic mixing, the DIPSI-2 sequence has superior performance over WALTZ-16 and should be used in any proton-proton TOCSY experiments. In addition, DIPSI-2 can be used to transfer either transverse (*Ix) or longitudinal magnetization (Iz) [139].*

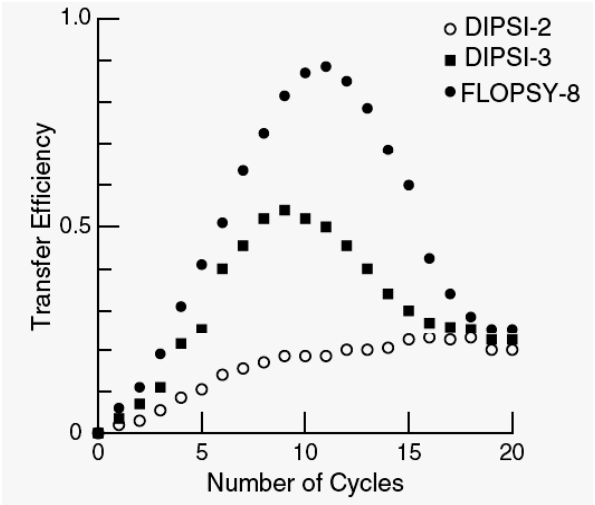

Figure 9.18 Transfer efficiency of DIPSI and FLOPSY sequences. *The* transfer efficiency of DIPSI-2, -3, and FLOPSY-8 is shown as a function of the mixing time. The sample was 13C labeled acetate, a B1 field strength of 7.93 kHz was used, and the transmitter was placed halfway between the C=O and methyl lines. The J-coupling constant for these two spins is 53 Hz, therefore 1/(2J) = 9.4 msec. Ten cycles corresponds to isotropic mixing times of 36.4 msec, 68.2 msec, and 29.7 msec, for DIPSI-2, DIPSI-3, and FLOPSY-8, respectively.

9.5.3 Time Dependence of Magnetization Transfer by Isotropic Mixing

The optimal transfer time can, in principle, be obtained from the transfer function:

$$sin^2(\pi J\tau)$$

In practice, the effective J-coupling between coupled spins depends on the frequencies of the two coupled spins relative to the transmitter. In general, as the frequency difference between the coupled spins increases the effective J-coupling decreases, therefore longer mixing times are required for optimal transfer. In the case of isotropic mixing using DIPSI-3, the effective J-coupling, $J_{effective}$, is approximately :

where θ is the angle between the spins in the rotating frame.

$$J_{effective} \approx J\left[1-(1-cos(\theta))\sqrt{\frac{8}{3}}\right]$$

Figure 9.19 Effective J-coupling during isotropic mixing. The effective J-coupling is obtained by multiplying the true J-coupling by the indicated correction factor. *δ* is the frequency difference between the position of the resonance line and the transmitter. *ν is the intensity of* the B1 field that is used for isotropic mixing. This plot assumes that the transmitter is placed half-way between the two coupled spins. For example, if a 10 kHz B1 field was used and the resonance lines for the coupled spins were 4 kHz apart, δ would be 2 kHz, and δ/ν would be 0.2, giving $J_{effective} \approx 0.87\ J$.

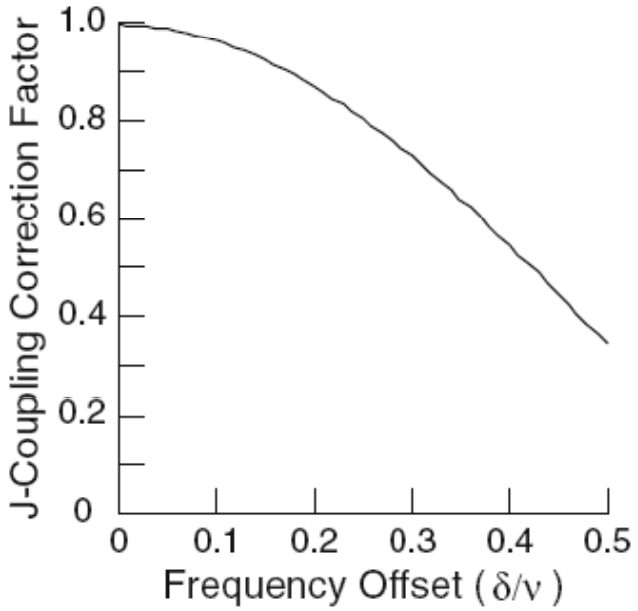

9.5.3.1 TOCSY Transfer Times in Amino Acids0

The time dependence of proton-proton transfer in alanine is shown in Fig. 9.20 and that for carbon-carbon transfer in threonine is shown in Fig. 9.21. Both figures show that it is possible to efficiently transfer magnetization to distant spins within the same residue (spin system). As anticipated from the size of the coupling constants, transfer of magnetization between coupled protons requires a longer mixing time than the transfer between coupled carbons. Consequently, the transfer of magnetization via proton-proton coupling will be relatively less efficient in larger proteins due to the shorter T2 relaxation time (Compare the right side of Fig. 9.20 to dashed lines on Fig. 9.21).

The secondary structure of a residue has a large effect on the ability to transfer magnetization from the amide proton to the side-chain. Residues in an a-helical conformation possess a small J-coupling between the amide and the Ha proton. This weak coupling greatly inhibits the transfer of magnetization from the amide proton to the remaining protons (compare the solid and dotted lines in Fig. 9.20). In contrast, since the carbon-carbon couplings are insensitive to secondary structure, the transfer of magnetization in carbon-carbon TOCSY is also insensitive to secondary structure.

In summary, a proton-proton TOCSY can be used to obtain a large number of correlations between the amide proton and the sidechain protons for smaller proteins, up to a size of ≈ 12-15 kDa. For proteins in the range of 20-25 kDa it would be possible to observe such cross peaks for residues in β-sheets. However, a poor signal-to-noise ratio may prevent the observation of transfers between distant spins, such as between the amide proton and the Hδ protons in isoleucine. In contrast, the transfer of carbon magnetization by isotropic mixing is much more robust than with protons due to the larger and more uniform carbon-carbon coupling constants.

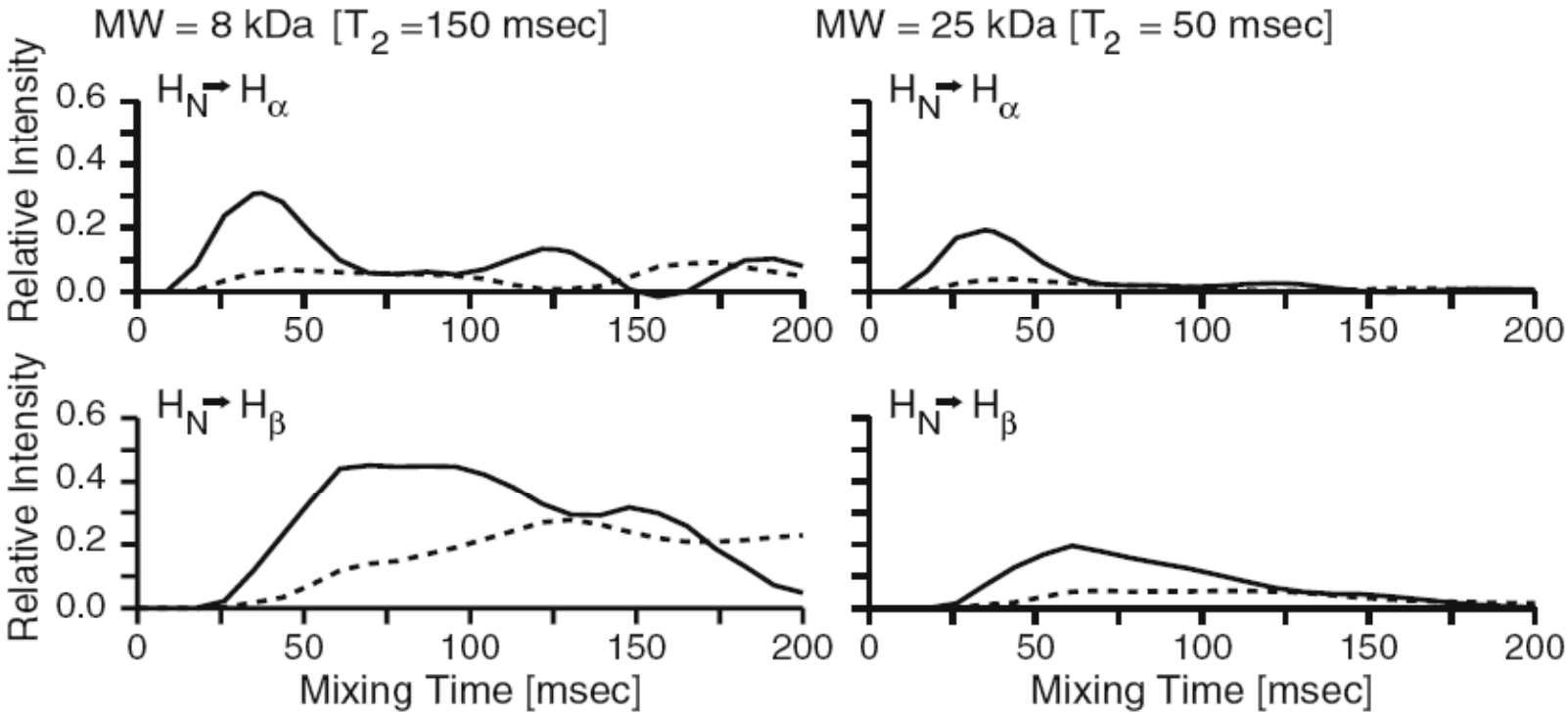

Figure 9.20. Effect of TOCSY mixing time on transfer efficiency. The effect of mixing time on the transfer of magnetization from the amide proton to the H_α proton (upper two panels) and H_β protons (lower two panels) of alanine are presented. The x-axis is the length of the isotropic mixing sequence, and the y-axis is the relative intensity of the crosspeak. The original intensity of the amide proton was 1.0. The solid line shows the transfer efficiency when $J_{HN-H\alpha}$ is 10 Hz (i.e. β-strand) and the dashed line shows the transfer efficiency when $J_{HN-H\alpha}$ is 4 Hz (i.e. α-helix). The left-hand panels show typical data for a $\approx$ 8 kDa protein and the right-hand panels represent transfer efficiencies for a $\approx$ 25 kDa protein. The transfer efficiencies, in the absence of relaxation, are from [29]. The effect of relaxation was simulated by multiplying the data by e^{-t/T_2}.

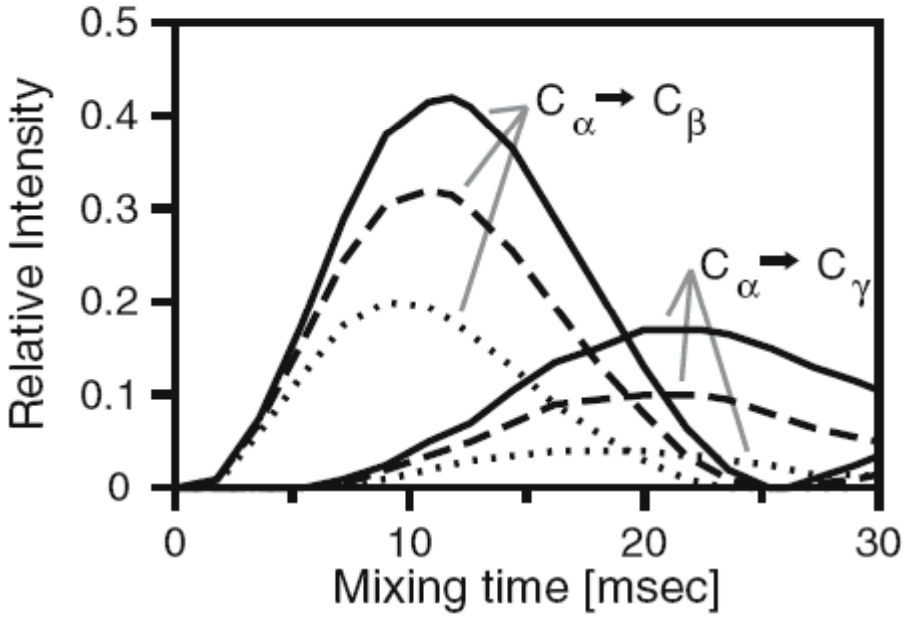

Figure 9.21 Carbon-carbon TOCSY transfer. The transfer rate of magnetization from the α-carbon of threonine to its β- or γ-carbon is shown for an 8 kDa (solid line), a 25 kDa (dashed line) or a 50 kDa protein (dotted line). The transfer efficiencies, in the absence of relaxation, were from Bax *et al* [9]: $J_{C\alpha C\beta} = 35$ Hz, $J_{C\beta C\gamma} = 19$ Hz. The effect of relaxation was simulated by multiplying the data by e^{-t/T_2}.